Journal of Alloys and Compounds 509 (2011) 4268–4272

Contents lists available at ScienceDirect

Journal of Alloys and Compounds

journal homepage: www.elsevier.com/locate/jallcom

Microstructure and hydrogen storage properties of Mg–Sn nanocomposite by mechanical milling

H.C. Zhong, H. Wang, L.Z. Ouyang, M. Zhu*

School of Materials Science and Engineering, South China University of Technology, Guangzhou 510640, PR China

ARTICLE INFO

Article history:
Received 30 June 2010
Received in revised form
10 November 2010
Accepted 11 November 2010
Available online 19 November 2010

Keywords:
Mg_2Sn/Mg nanocomposite
Hydrogen storage properties
Mechanical alloying

ABSTRACT

To improve the hydrogen storage properties, the composition and microstructure of Mg–Sn alloys were modified through fabricating Mg/Mg_2Sn nanocomposite by mechanical alloying. The microstructures were characterized by X-ray diffraction and scanning electron microscopy. It is found that Mg_2Sn instead of Mg(Sn) solid solution is preferably formed during milling process. Although Mg_2Sn is not a hydriding phase, the in situ formed nanosized Mg_2Sn facilitates hydrogen absorption/desorption of Mg by forming Mg/Mg_2Sn nanocomposite. The mechanically milled Mg–5 at.% Sn nanocomposite exhibits slightly elevated plateau pressure and destabilized thermodynamics due to the introduction of large amount of interface energy in Mg/Mg_2Sn nanocomposite.

1. Introduction

Magnesium hydride (MgH_2) is regarded as a promising solid-state hydrogen storage material for its large capacity (7.6 wt.%), excellent cyclability and low cost. However, the unacceptable high decomposition temperature and sluggish kinetics seriously restrict its practical applications. Intensive efforts have been devoted to overcoming these barriers and great progresses have been achieved in the past decades. Tremendous research work can be summarized as follows: (1) Modifying microstructure and composition by preparing Mg-based alloys or solid solutions [1–3]. Fernández et al. found that the $Mg_{90}Ni_{10}$ and $Mg_{80}Ni_{10}Y_{10}$ alloys showed enhanced kinetics at a drastically lowered temperature of 473 K. For $Mg_{90}Ni_{10}$, the improved kinetics were attributed to the catalytic effect of $Mg_2NiH_{0.3}$, while the dissolving of Y in Mg_2Ni was responsible for fast hydrogen desorption of $Mg_{80}Ni_{10}Y_{10}$ [1]. (2) Doping catalysts, such as metals or the mixtures of metals and carbon nanotube, or intermetallic compound [4–7]. For instance, the Mg–Fe–Ti thin film showed fast sorption kinetic and low desorption temperature of 473 K [4]. The synergistic catalytic effect of Fe and Ti facilitated hydrogen dissociation/reassociation and diffusion in the magnesium; Recent study also showed that the addition of Mg_2Ni helped to lower the desorption temperature of MgH_2 from 603 to 463 K, and substantially improved kinetics were achieved when doping the mixture of Mg_2Ni and TiH_2 [7]. (3) Fabricating nanostructured Mg or MgH_2, the reduction of grain/particle size not only improves the kinetics but also decreases the thermodynamic stability of MgH_2 [8–10]. (4) Constructing new system through compositing with other hydrogen storage materials. For example, the nanocrystalline Mg + x wt.% $LaMg_2Ni$ (x = 0–30) composites showed excellent hydriding performance and fairly lower desorption temperature of 453 K [11]. In addition, synthesizing novel magnesium hydrides under ultrahigh pressure or new magnesium-based alloys by ball milling technique are also important approaches. For example, the FCC structured $Mg_{7-x}A_xTiH_{16-x}$ (A = Li, Na, K, x = 0–1) and Mg–TM (TM = transition metal: Ti, Co or Ni) BCC alloys are all potential hydrogen storage materials [12,13].

Some earlier work showed that addition of Sn played positive effect to the hydrogen desorption properties of Mg and Mg-based alloys. For instance, the mechanically milled Sn/MgH_2 nanocomposite showed substantially lowered desorption temperature [14], and similar effect was found in the Ge/MgH_2 nanocomposite [15]. By investigating the electron structure and charge density of MgH_2, Chen et al. found that Mg–H bond could be weakened by partial substitution of Sn for Mg [16]. From the Mg–Sn binary phase diagram [17], the equilibrium solubility of Sn in Mg is negligible below 573 K, also Sn does not dissolve in Mg lattice. There exist two eutectic reactions involving the Mg/Mg_2Sn and Mg_2Sn/Sn mixtures. Recently, Urretavizcaya and Meyer reported that the cubic Mg_2Sn could transform to the metastable hexagonal Mg_2Sn by milling Mg and Sn mixture in Ar or hydrogen atmosphere [18]. It is believed that Mg_2Sn might play catalytic role to the hydrogen absorption/desorption of Mg because similar effect was demonstrated in the eutectic mixtures of Mg/Mg_2Ni [19]. On the other hand, considering the fact that Mg and Sn atoms have favorable size factor, the solubility of Sn in Mg could be possibly extended

* Corresponding author. Tel.: +86 20 87113924; fax: +86 20 87111317.
E-mail address: memzhu@scut.edu.cn (M. Zhu).

0925-8388/$ – see front matter © 2010 Elsevier B.V. All rights reserved.
doi:10.1016/j.jallcom.2010.11.072

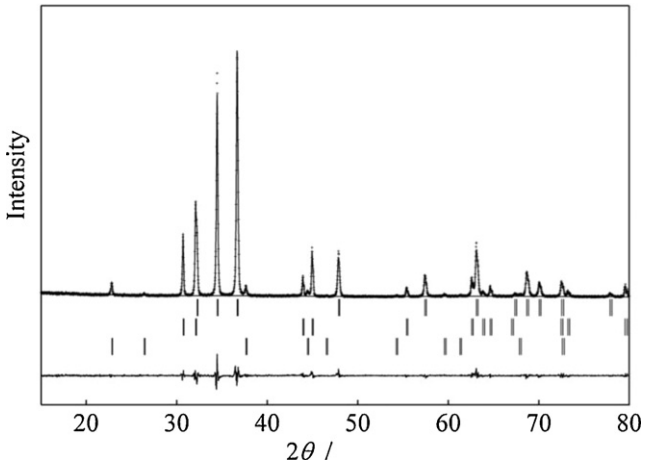

Fig. 1. Rietveld refinement of the observed XRD pattern for Mg–2 at.% Sn milled for 6 h. Measured (dots), calculated (upper line), and difference curve (lower line) are shown. Vertical bars (from above) are Mg, Sn and Mg_2Sn Bragg diffractions, respectively.

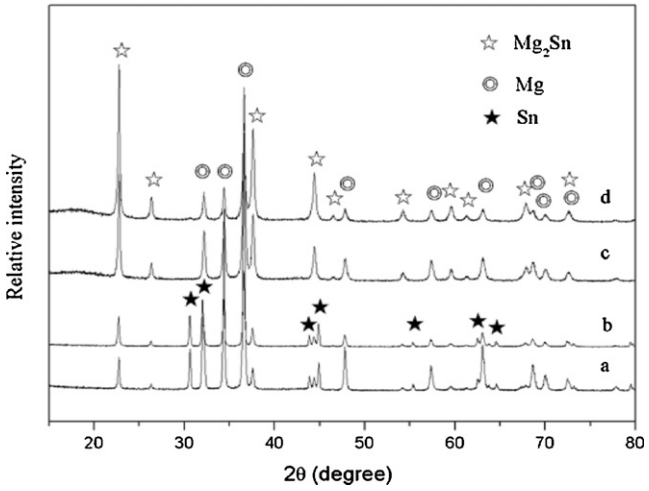

Fig. 2. XRD patterns for Mg–2 at.% Sn (a, c) and Mg–5 at.% Sn (b, d) respectively milled for 20 h (a, b) and 60 h (c, d).

by mechanical milling and the formation of Mg(Sn) solid solution might improve the hydrogen storage properties because Sn has weaker affinity to H than Mg.

Based on above considerations, in this work, we attempted to prepare Mg(Sn) solid solution and Mg/Mg_2Sn composite by mechanical milling, which has been widely used to synthesize novel hydrogen storage materials. The microstructures and hydrogen storage properties of Mg–Sn composites were investigated in detail.

2. Experimental details

Mg and Sn powders with purity of 99.9% and size of 200 mesh were used as starting materials. The Mg–Sn powder mixtures with designed composition (Mg–2 at.% Sn, Mg–5 at.% Sn), together with stainless steel balls, were sealed in the stainless steel vials in a glove box filled with pure Ar. The ball-to-powder mass ratio is 20:1. The ball milling was performed on a QM-3SP2 planetary mill with rotation speed of 200 rpm. To prevent over rising of temperature, the milling was interrupted for 30 min after every 30 min of milling.

Phase analysis was performed by powder X-ray diffraction (XRD) on a Philips X'Pert diffractometer with Cu Kα radiation (λ = 1.54060 Å). The zero shift of diffractometer was calibrated using high purity silicon (99.999%). Lattice constants and phase abundance were calculated by Rietveld method using Rietan 2000 program [20]. Scanning electron microscope (SEM, NOVA NANOSEM 430) was used to observe the morphology and phase distribution.

The hydrogen absorption/desorption kinetics and pressure-composition-isothermals (PCI) were measured by an automatic Sieverts apparatus (Advanced Materials Inc.). The starting hydrogen pressure was set as 2.5 MPa for hydrogen absorption kinetics test. Hydrogen desorption was carried out in vacuum condition at 573 K. The delay time for PCI measurement was set as 40 s.

3. Results and discussion

3.1. Microstructure of Mg–Sn composites

Fig. 1 shows the Rietveld analysis profile of Mg–2 at.% Sn milled for 6 h. The fitting indices of pattern *R*-factor (R_p), weighted pattern *R*-factor (R_{wp}) and goodness-of-fit (*S*) are 8.2%, 11.2% and 1.2, respectively, indicating that the calculated pattern well matches the experimental pattern in the entire scanning range. Besides the Mg and Sn phases, Mg_2Sn is identified with weight percentage of about 1 wt.%. To investigate whether Sn is dissolved in Mg, the lattice constants and phase abundance of samples milled for 1, 3 and 6 h were evaluated by Rietveld refinement. The results show that the lattice constants of Mg experience a negligible change, but the abundance of Mg_2Sn continuously increases with extension of milling time. It indicates that extending the solubility of Sn in Mg by mechanical milling is not feasible, which is not like the Mg–Ti system [21]. One important reason is the preferred formation of Mg_2Sn, which restricts the dissolving of Sn into Mg lattice. With the proceeding of milling, the added Sn can completely react with Mg, and only Mg and Mg_2Sn are present (Fig. 2c and d). Also, phase quantitative analysis reveals that the weight percentage of Mg_2Sn in 60 h-milled Mg–2 at.% Sn (Fig. 2c) and Mg–5 at.% Sn (Fig. 2d) is about 11 wt.% and 28 wt.%, respectively, which are close to the theoretical values of 12.8 wt.% and 28.8 wt.%.

As shown in Fig. 2, the diffraction peaks of Mg and Mg_2Sn are gradually broadened with prolonging milling time, indicating grain refinement caused by milling. By Scherrer equation, the crystallite size of Mg and Mg_2Sn were roughly calculated using the full width at half maximum of Mg (0 0 0 2) and Mg_2Sn (2 0 0) peaks, and their evolution with milling time is shown in Fig. 3. Besides nanocrystalline Mg_2Sn with crystallite size of about 40 nm, the crystallite size of Mg in Mg–2 at.% Sn and Mg–5 at.% Sn composites was quickly decreased down to about 75 nm, and then gradually reduced to approximate 45 nm. However, our experiments revealed that pure Mg was difficult to be refined to nanocrystalline just by milling in Ar atmosphere. Therefore, it can be concluded that the formation of Mg_2Sn facilitates the grain refinement of Mg. We also noticed that

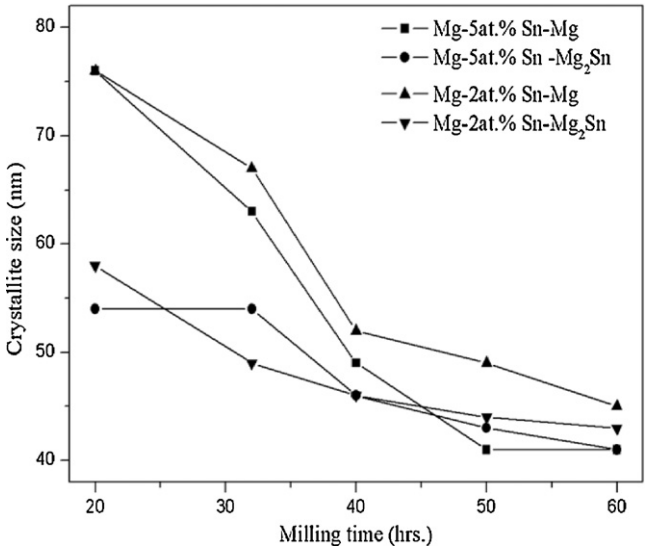

Fig. 3. Crystallite size of Mg and Mg_2Sn as function of milling time.

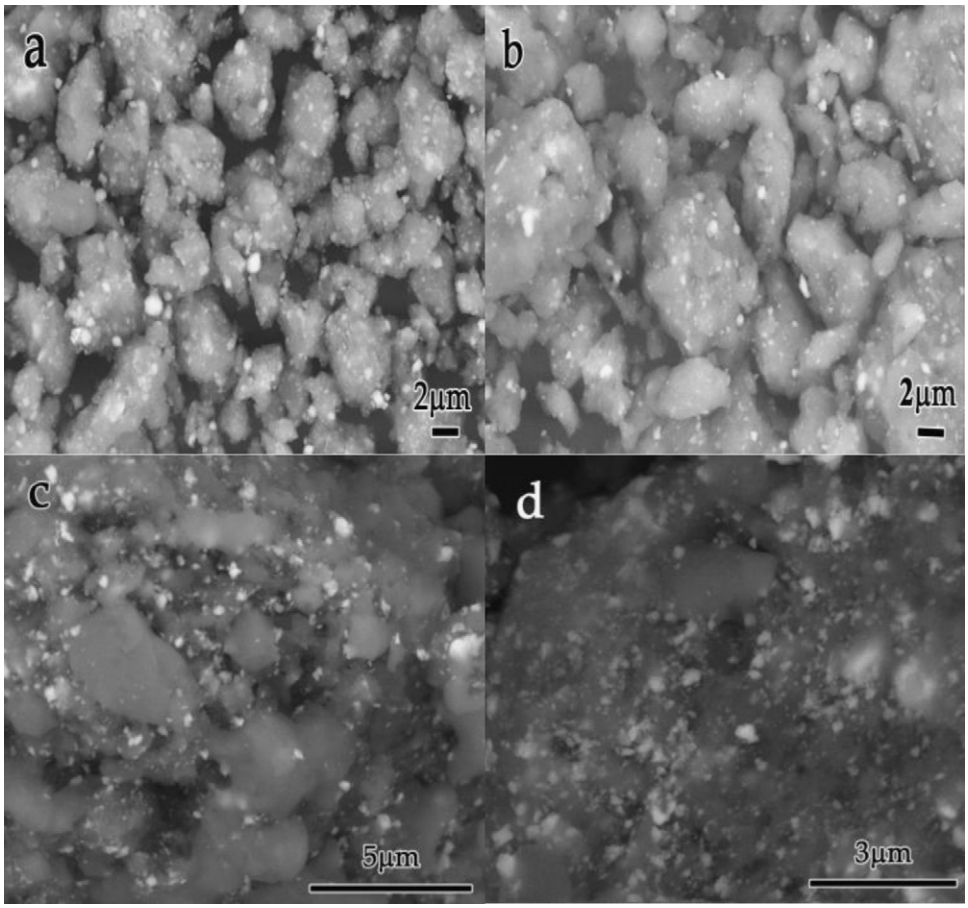

Fig. 4. XRD patterns of Mg–5 at.% Sn nanocomposite. (a) As-hydrogenated and (b) as-dehydrogenated.

Mg crystallites grew up to greater than 100 nm after 5 hydrogen absorption/desorption cycles, whereas Mg_2Sn remained nanocrystalline structure, which was attributed to it's dispersive distribution in Mg matrix as shown in Fig. 4. The back scattering SEM images of as-prepared and dehydrogenated Mg–2 at.% Sn and Mg–5 at.% Sn composites were displayed in Fig. 4. It is seen that nanosized Mg_2Sn particles/grains (bright parts) are dispersively embedded in the Mg matrix (gray parts).

Fig. 5 shows the XRD patterns of hydrogenated and dehydrogenated Mg–5 at.% Sn composite. Apart from the presence of Mg, MgH_2, Mg_2Sn, any kinds of Mg_2Sn–H phase are not observed, suggesting that Mg_2Sn is not a hydriding phase. This result is in agreement with previous work [22]. To further investigate the formation and hydriding properties of Mg_2Sn, we prepared the Mg_2Sn compound by milling the Mg–33.3at.% Sn powder mixtures. Both cubic Mg_2Sn and hexagonal Mg_2Sn were obtained (Fig. 6). The metastable hexagonal Mg_2Sn is normally

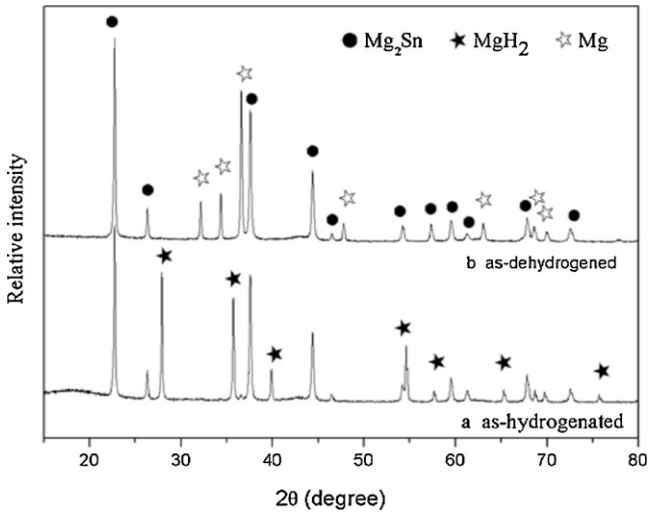

Fig. 5. Back scattering SEM images of as-prepared Mg–2 at.% Sn (a) and Mg–5 at.% Sn (b), dehydrogenated Mg–2 at.% Sn (c) and Mg–5 at.% Sn (d).

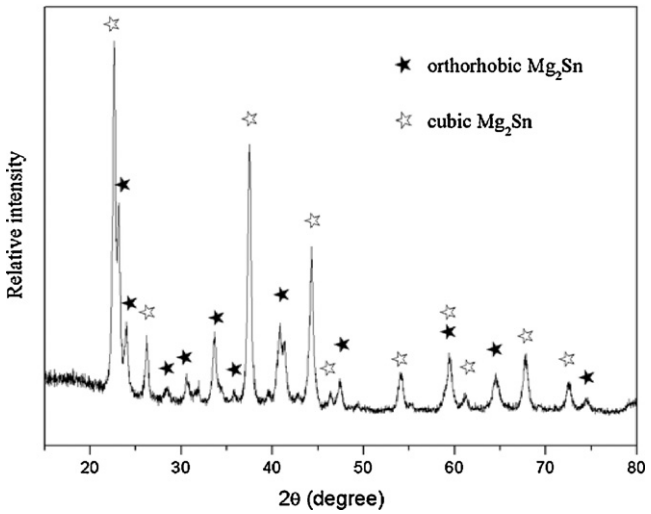

Fig. 6. XRD pattern of mechanically milled Mg–33.3 at.% Sn powder mixture.

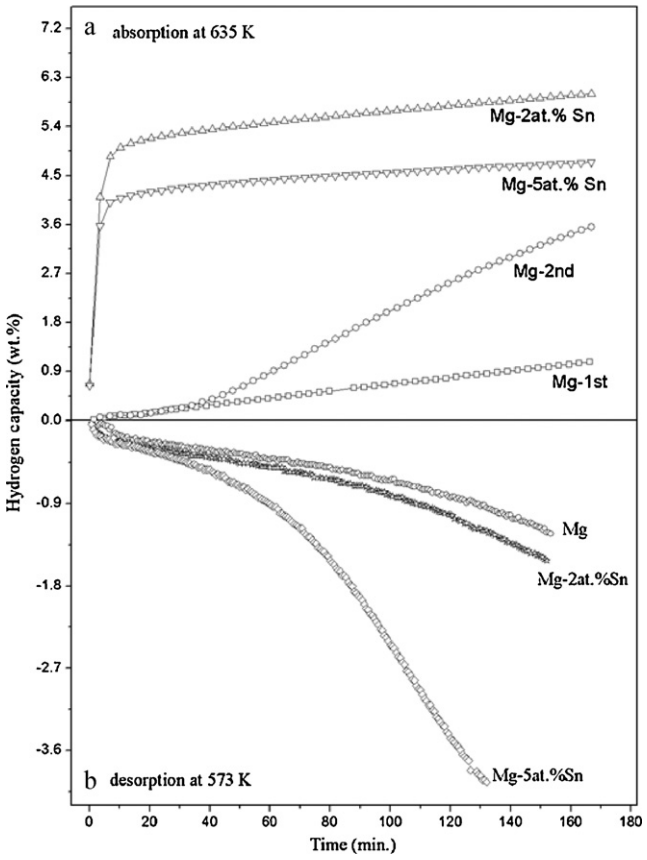

Fig. 7. Hydrogen absorption (a) and desorption (b) kinetic curves of pure Mg, Mg–2 at.% Sn and Mg–5 at.% Sn nanocomposites. Mg-1st and Mg-2nd represent the first and second hydrogen absorption for Mg, respectively.

synthesized under high-pressure and high-temperature conditions. The formation of hexagonal Mg_2Sn at room temperature could be related to the gigantic stress caused by milling [18]. The as-prepared Mg_2Sn compound was hydrogenated at 653 K and under 4 MPa hydrogen pressure for 24 h. No significant hydrogen uptake was observed, further confirming that both cubic Mg_2Sn and hexagonal Mg_2Sn are not suitable for hydrogen storage.

3.2. Hydrogen sorption/desorption properties of Mg–Sn composite

Fig. 7 shows the hydrogen absorption/desorption kinetics at 653 K of Mg–2 at.% Sn and Mg–5 at.% Sn milled for 60 h, together with 60 h-milled pure Mg for comparison. Mg showed fairly sluggish kinetics at the first/second hydrogen absorption cycle, which should be related to the MgO layer on the surface of Mg particles. The passive MgO layer impedes hydrogen adsorption, dissociation and diffusion to the inner of particles and has to be broke down by annealing in hydrogen atmosphere prior to rapid hydrogen absorption. Actually, after full activation, pure Mg shows rapid hydriding speed at this temperature. In comparison, both Mg–2 at.% Sn and Mg–5 at.% Sn nanocomposites exhibited greatly improved hydrogen absorption kinetics, absorbing more than 4 wt.% hydrogen in 10 min at the first hydrogen absorption. Enhanced hydrogen desorption kinetics is also found in the Mg–5 at.% Sn nanocomposite. We believe that two microstructural characteristics are responsible for the kinetic improvement of Mg. First, abundant grain/phase boundaries in the Mg–Sn nanocomposites can facilitate hydrogen sorption by providing hydrogen diffusion channels and stable nucleation sites for MgH_2. Second, the existence of Mg_2Sn possibly

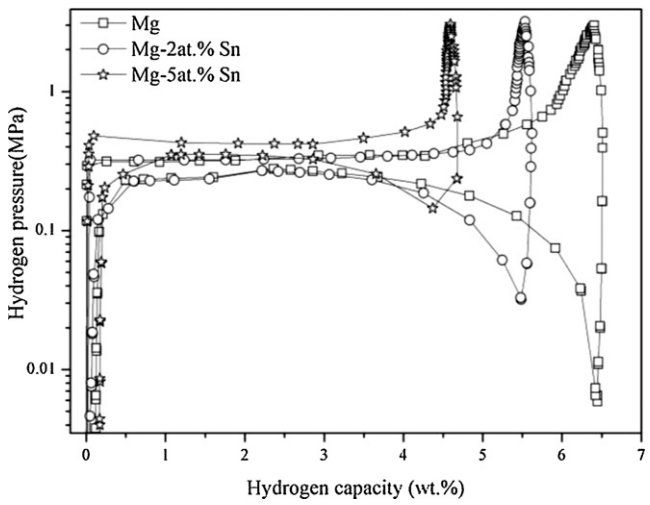

Fig. 8. PCI curves at 596 K for Mg, Mg–2 at.% Sn and Mg–5 at.% Sn.

prevents the formation of continuous MgO layer and thus enhances the absorption/desorption kinetics of Mg.

The comparison in pressure-composition-isotherms at 596 K for Mg, Mg–2 at.% Sn and Mg–5 at.% Sn is shown in Fig. 8. Besides the capacity difference, different hydrogen desorption hysteresis and plateau pressure can be observed. It is noted that all the three alloys show lag in desorption curves and the Mg–5 at.% Sn has the smallest lag. This also indicates that Mg–5 at.% Sn composite has the best desorption kinetic. Furthermore, the plateau pressure of Mg–5 at.% Sn shows obvious increase in comparison with that of pure Mg and Mg–2 at.% Sn, implying a lower temperature is required to obtain an equilibrium pressure of 1 bar H_2 than that for pure MgH_2. The thermodynamic properties are further evaluated by the enthalpy change (ΔH) and entropy change (ΔS) of hydrogen desorption, which could be estimated by the van't Hoff equation:$\ln\left(\frac{P_H}{P_0}\right) = \frac{\Delta H}{RT} - \frac{\Delta S}{R}$ where P_H is the equilibrium pressure, P_0 is the standard atmospheric pressure and R is the gas constant. The van't Hoff plots for Mg, Mg–2 at.% Sn and Mg–5 at.% Sn nanocomposites are shown in Fig. 9. The calculated ΔH for Mg, Mg–2 at.% Sn and Mg–5 at.% Sn nanocomposites are 77.9 ± 0.3, 77.4 ± 0.9 and 75.2 ± 0.7 kJ mol^{-1} H_2, and the ΔS are 138.9 ± 0.6, 138.2 ± 1.2 and 136.5 ± 1.0 J mol^{-1} K^{-1} H_2, respectively. It is seen that ΔH and ΔS of pure Mg are slightly greater than the com-

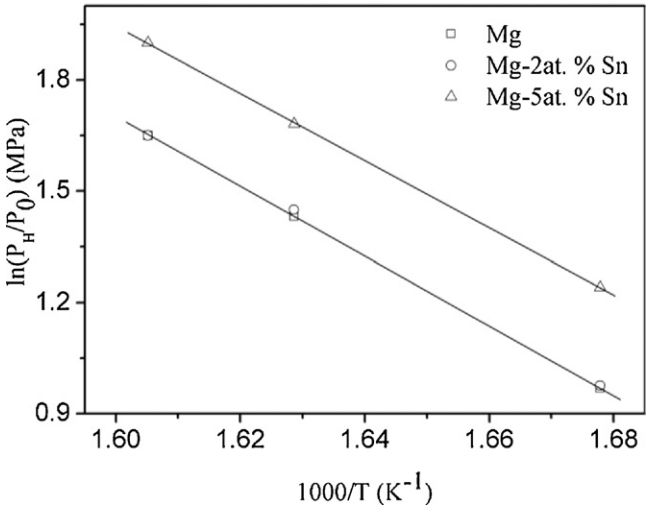

Fig. 9. van't Hoff plots of Mg–2 at.% Sn and Mg–5 at.% Sn in comparison with that of Mg.

monly accepted as a reference (74.7 kJ mol^{-1} H_2, 130 J mol^{-1} K^{-1} H_2) [23], which should be related to the experimental error in this study. As expected, in comparison to pure Mg, there is a negligible enthalpy change for Mg–2 at.% Sn but measurable reduction of enthalpy change for Mg–5 at.% Sn. The decrease in ΔH should be related to the nanocomposite structure. Previous work has proved that nanocrystalline Mg or Mg_2Ni alloy has lower ΔH and ΔS than that of bulk Mg due to the introduction of extra interface energy [24]. Therefore, sufficient nanosized Mg_2Sn existing in the Mg–5 at.% Sn nanocomposite will lead to greater interface energy and ΔH decrease comparing with Mg–2 at.% Sn nanocomposite.

It should be also noted that ΔS of Mg–5 at.% Sn nanocomposite experiences slight decrease by 2.4 J mol^{-1} K^{-1} H_2 in comparison to pure Mg. It is generally accepted that the entropy change of hydrogen desorption of metal hydrides is a constant value, which is not dependent on the microstructure of hydrides, including nanocrystalline hydrides. Although some work reported increased or decreased entropy changes [25,26], but the reason was not given. Recently, Paskevicius et al. deliberately measured the thermodynamic changes in magnesium hydride nanoparticles with about 7 nm in size, which showed ΔH decrease of 2.84 kJ mol^{-1} H_2 as well as ΔS decrease of 3.8 J mol^{-1} K^{-1} H_2 [9]. Since the reaction entropy upon $MgH_2 \rightarrow Mg + H_2$ can be expressed as $S_{Mg} + S_{H_2} - S_{MgH_2}$, where S_{H_2} is the configuration entropy of hydrogen molecule, if the entropy of MgH_2 increases by a greater quantity than the entropy for Mg as particle size is reduced, a lower ΔS will be generated. Similar reason can be applied to the studied Mg–Sn nanocomposite. Upon dehydrogenation, MgH_2/Mg_2Sn interface changes into Mg/Mg_2Sn interface, which might cause a negative ΔS because the Mg/Mg_2Sn interface seems to be more ordered than MgH_2/Mg_2Sn interface, but more evidences are required to support this point. Obviously, the decrease in ΔS will partially counteract the destabilization effect from the reduction in ΔH, but ΔH has greater effects on the change of desorption temperature.

4. Conclusions

In this paper, the microstructure and hydrogen storage properties of Mg–Sn nanocomposite by mechanical milling were investigated. It is found that the dissolving of Sn in Mg lattice is negligible due to the preferential formation of Mg_2Sn. However, the addition of Sn promotes the grain refinement of Mg due to the formation of Mg_2Sn. However, Mg_2Sn is not a hydriding phase which is not suitable for hydrogen storage. But the mechanically milled Mg/Mg_2Sn nanocomposites show improved hydrogen absorption/desorption kinetics as well as destabilized thermodynamics.

Acknowledgements

This work was financially supported by the National Natural Science Foundation of China under Grant No. 50631020, the Ministry of Science and Technology under project 2010CB631302, and the Fundamental Research Funds for the Central Universities-SCUT.

References

[1] J.F. Fernández, F. Cuevas, F. Leardini, et al., J. Alloys Compd. 495 (2010) 663–666.
[2] S. Kalinichenka, L. Rntzsch, C. Baehtz, B. Kieback, J. Alloys Compd. 496 (2010) 608–613.
[3] T.Z. Si, Y.F. Liu, Q.A. Zhang, J. Alloys Compd. 507 (2010) 489–493.
[4] C. Harrower, E. Poirier, H. Fritzsche, P. Kalisvaart, S. Satija, B. Akgun, D. Mitlin, Int. J. Hydrogen Energy 35 (2010) 10343–10348.
[5] X.D. Yao, C.Z. Wu, A.J. Du, J. Zou, Z.H. Zhu, P. Wang, H.M. Cheng, S. Smith, G.Q. Lu, J. Am. Chem. Soc. 129 (50) (2007) 15650–15654.
[6] B. Zahiri, C.T. Harrower, B.S. Amirkhiz, D. Mitlin, Appl. Phys. Lett. 95 (2009) 103114–103117.
[7] S.T. Sabitu, G. Gallo, A.J. Goudy, J. Alloys Compd. 499 (2010) 35–38.
[8] W.Y. Li, C.S. Li, H. Ma, J. Chen, J. Am. Chem. Soc. 129 (2007) 6710–6711.
[9] M. Paskevicius, D.A. Sheppard, C.E. Buckley, J. Am. Chem. Soc. 132 (2010) 5077–5083.
[10] S. Barcelo, M. Rogers, C.P. Grigoropoulos, S.S. Mao, Int. J. Hydrogen Energy 35 (2010) 7232–7235.
[11] X.Z. Xiao, G.C. Liu, S.K. Peng, K.R. Yu, S.Q. Li, C.P. Chen, L.X. Chen, Int. J. Hydrogen Energy 35 (2010) 2786–2790.
[12] T. Takasaki, T. Mukai, N. Kitamura, S. Tanase, T. Sakai, J. Alloys Compd. 494 (2010) 439–445.
[13] H.Y. Shao, K. Asano, H. Enoki, E. Akiba, J. Alloys Compd. 477 (2009) 301–306.
[14] H. Imamura, K. Tanaka, I. Kitazawa, T. Sumi, Y. Sakata, N. Nakayama, S. Ooshima, J. Alloys Compd. 484 (2009) 939–942.
[15] F.C. Gennari, F.J. Castro, G. Urretavizcaya, G. Meyer, J. Alloys Compd. 334 (2002) 277–284.
[16] D. Chen, L. Chen, Y.M. Wang, S. Liu, Rare Metal Mater., Eng. 33 (2004) 485–489.
[17] A.A. Nayeb-Hashemi, J.B. Clark, Massalski International ASM Binary Phase Alloy Diagrams, 2nd ed., American Society or Metals, Metals Park, OH, 1996.
[18] G. Urretavizcaya, G.O. Meyer, J. Alloys Compd. 339 (2002) 211–215.
[19] K. Nogita, S. Ockert, J. Pierce, M.C. Greaves, C.M. Gourlay, A.K. Dahle, Int. J. Hydrogen Energy 34 (2009) 7686–7691.
[20] F. Izumi, T. Ikeda, Mater. Sci. Forum 198 (2000) 321–324.
[21] G. Liang, R. Schulz, J. Mater. Sci. 38 (2003) 1179–1184.
[22] R. Janot, F. Cuevas, M. Latroche, A. Percheron-Guégan, Intermetallics 14 (2006) 163–169.
[23] K. Bohmhammel, U. Wolf, G. Wolf, E. Konigsberger, Thermochim. Acta 337 (1999) 195–199.
[24] L.Z. Ouyang, S.Y. Ye, H.W. Dong, M. Zhu, Appl. Phys. Lett. 90 (2007) 021917–021919.
[25] A. Andreasen, Int. J. Hydrogen Energy 33 (2008) 7489–7497.
[26] Y.P. He, Y.P. Zhao, Nanotechnology 20 (2009) 204008–204018.